Point Defects Control Guest Molecule Diffusion in the 1D Pores of Zn(tbip)

Xuqing Cai[1], David S. Sholl[1,2]*

[1]School of Chemical & Biomolecular Engineering

Georgia Institute of Technology, Atlanta, GA 30332, United States

[2]Oak Ridge National Laboratory, Oak Ridge, TN 37830, United States

Abstract

Molecular diffusion plays a critical role in metal-organic frameworks (MOFs) within application of kinetic chemical separations. We carefully study in this work the unexpected role of point defects for short-chain alkanes diffusing in Zn(tbip), a MOF with rigid 1D channels. Inside a defect-free Zn(tbip), guest molecules are expected to follow single-file diffusion along 1D channels. It has been found previously by Heinke et al. that these parallel 1D channels are connected for molecular diffusion. Our Density-Functional Theory (DFT) calculations suggest that linker vacancy defects could arise under experimentally-relevant conditions by removing a pair of linkers. Further climbing-image Nudged Elastic Band (cNEB) DFT calculations indicate that hopping of short-chain alkanes between adjacent 1D channels over defect windows can happen under moderate temperature. In addition to providing insights into connected adjacent 1D

channels in Zn(tbip), Heinke et al. also inferred most 1D pores are blocked from their microkinetic model. We also explored influence of hydrolyzed linker created by the formation of linker removal inside 1D pores. Our DFT calculations show the linkers can effectively block the pores and the linker diffusion in 1D channels are slow. Our results, for the first time, offer a mechanistic explanation of previous uncommon molecular diffusion behavior in this MOF with 1D channels.

Introduction

Metal-organic frameworks (MOFs) are a subclass of nanoporous materials with high surface areas and chemically diverse structures.[1] The strong chemical tunability and properties such as open metal site in MOFs can lead to high selectivity for adsorption of certain chemicals.[2-4] Although MOFs are crystalline materials, defects are expected to be ubiquitous in the pores of MOFs even under well controlled synthesis conditions.[5, 6] The identity and impact of these defects varies among materials and applications. For example, three commonly used MOF structures, HKUST-1, UiO-66 and ZIF-8 have been shown to contain defect sites.[7-9] In UiO-66 two types of defects, missing BDC (benzene-1,4-dicarboxylate) linkers and missing clusters can exist.[10]. A computational characterization of ZIF-8 defects was presented by Zhang et al.,[11] including missing linkers, missing metals and a "dangling linker" defect where a part of linker is removed and terminated with other groups. Isolated defects induced by acid gas environments in zeolite imidazolate frameworks (ZIFs), can lead to crystal structure degradation.[12, 13] Extended defects can also exist in MOFs. Han et al. used modeling to illustrate extended defects in ZIFs that are analogous to stacking faults, a type of intergrowth disorder known to exist in a number of zeolites.[14, 15]

Experimental approaches have been developed to deliberately create defects in MOFs via so-called defect engineering.[16, 17] Shearer et al. presented a useful description of the defect chemistry of UiO-66 when this MOF is synthesized with appropriate modulators.[18, 19] Related work on UiO-66 defect engineering has shown how modulator addition during synthesis can enhance thermal stability.[20]

Diffusion of molecules inside MOFs is important in a number of settings, including the separation of molecules by kinetic separations and in membrane-based separations. Molecular simulations have been widely used to predict molecular diffusivities in MOFs, but these simulations are almost without exception based on pristine, defect-free crystal structures.[21, 22] Little is known about the possible impacts of defects on intramolecular diffusion in MOFs.[23] Han et al. modeled molecular diffusion in ZIF-8 that contained isolated defects associated with degradation by acid gases and concluded that defects would have a negligible impact on net diffusion in the 3D pores of these materials.[24] It is not clear, however, how generalizable this conclusion is. Some recent studies focused on molecular interactions in porous media by controlling defect concentration. A follow-up study led by Heinke et al. used surface-mounted MOFs with adjustable defect density as model systems for molecular diffusion.[25] Another recent work by Llewellyn and his co-workers focused on propane/propylene separation using MOF-801 through defect engineering.[26] They used Grand Canonical Monte Carlo (GCMC) simulations to suggest that missing cluster defects in this MOF increase diffusivities rates of propane and propylene.

In this paper we focus on the diffusion of molecules in a specific MOF, Zn(tbip) (tbip = 5-*tert*-butyl isophthalate). Understanding the details of molecular diffusion in this specific material helps to explain some puzzling aspects of previous experiments and also gives hints about how defects may play a role in molecular diffusion in a wider class of nanoporous materials. Zn(tbip) was first reported by Pan et al. to be a thermally stable guest-free MOF with a pore diameter of 4.5 Å that has potential to separate dimethyl ether (DME) and methanol.[27] The pores inside a defect-free Zn(tbip) crystal are one dimensional (1D). This situation is not unusual. Simon et al.

selected a diverse set of 3640 experimentally reported MOF structures from the Nanoporous Material Genome database using a feature space of density, surface area, pore limiting diameter (PLD) and void fraction to find materials to separate Xe/Kr mixtures.[28] They split the MOF dataset into structures with 1D cylinder-like channels and structures with 2D and 3D channels and showed the number of 1D channel MOFs are comparable to that of 2D and 3D MOFs.

For adsorbed molecules that are comparable in size to the pores in which they are adsorbed, diffusion inside 1D channels will be single-file, which means they cannot pass through each other inside the 1D channels. A prominent example of single-file diffusion is in molecular sieve $AlPO_4$-5. $AlPO_4$-5 has nonintersecting quasi-cylindrical pores with diameter of 7.3 Å, which makes it useful to understand single-file diffusion.[29] Gupta et al. experimentally measured diffusion of ethane in large crystal of $AlPO_4$-5 with long longitudinal relaxation times and found the mean square displacement was proportional to the square root of time, thus providing direct evidence of single-file diffusion in this material.[30]

Motivated in part by previous examples of single-file diffusion, Heinke et al. used transient concentration profiles for sorption and tracer exchange via IR microimaging in Zn(tbip) to measure transport and self-diffusivities of short-chain alkanes from ethane to *n*-butane.[31] Their results gave strong evidence that propane diffusion in Zn(tbip), contrary to expectations based on the pore size, did not follow a single-file diffusion behavior. The microscopic origin of this observation remains unknown. Additional experiments by Heinke and Karger suggested another surprising feature of molecular diffusion in Zn(tbip), namely that the transport rate of guest molecules in Zn(tbip) is controlled by resistances at the external surface instead of

intracrystalline diffusion.[32] A phenomenological model incorporating these so-called surface resistances based on these experiments predicted that only one out of 2000 external pores of the crystal surface was unblocked and allowed molecules to enter and exit.[33] As in most other analyses of molecular diffusion that imply the existence of surface barriers, no microscopic description of the origin of these barriers has been proposed.[34-37]

In this paper, we use atomistic models to explore the molecular diffusion of several alkane species in Zn(tbip). A key outcome from these models is that defects in Zn(tbip) play a pivotal role in molecular diffusion in this MOF. We show that the lack of single-file diffusion observed experimentally can be understood in terms of physically plausible defects that allow facile hopping of adsorbed molecules between adjacent 1D pores. Moreover, our results suggest that the surface barriers mentioned above are not truly surface effects, rather, they are associated with pore blockages associated with linkers in Zn(tbip) that have formed point defects but remain in the material's 1D pores.

Methods

Spatially periodic Density Functional Theory (DFT) calculations were performed using the Vienna Ab initio Simulation Package (VASP) with D3 dispersion corrections[38] and the Perdew-Burke-Ernzerhof exchange-correlation functional.[39] The Zn(tbip) conventional unit cell file was obtained from Cambridge Structural Database (CSD), which was then converted into a triclinic primitive cell with P1 space group that contains 348 atoms and a lattice constant of 17.48 Å. Geometry optimization using a conjugate gradient method and an energy cutoff of 520 eV was performed on pristine Zn(tbip) with relaxation of both lattice parameters and ionic positions until

interionic forces reached less than 0.01 eV/Å. The optimized lattice parameter was 17.54 Å, very similar to the experimental value. The optimized pristine Zn(tbip) unit cell was used to construct defective structures. Calculations with the defective structures used fixed lattice parameters but allowed all atom positions to relax unless otherwise noted. A 1×1×1 k-point mesh was used for all calculations. The climbing Nudged Elastic Band (cNEB) method is used to quantify energy barriers for hopping of molecules between local energy minima in pristine and defective Zn(tbip).[40, 41]

Results and Discussion

The crystal structure for Zn(tbip) reported by Pan et al.[27] contains one-dimensional cylinder-like channels with a pore diameter of 4.5 Å, which suggests one guest molecule will fill most of the 1D channels and prevent other molecules from passing through. We first calculated the binding energies relative to the gas phase for C_2H_6, C_3H_8 and *n*-C_4H_{10} in pristine Zn(tbip) by energy minimization of each adsorbed molecule. As shown in **Table 1**, the binding energy increases as the molecule's size increases due to the larger number of interactions between adsorbates and the framework. We also computed the energy barrier for molecular diffusion of each isolated molecule in the pristine material using cNEB calculations (see **Table 1**). This energy barrier increases as the molecular size of the adsorbate increases, but each barrier is low enough that this kind of diffusion will occur readily at room temperature. We attempted to perform cNEB calculations for the passage of propane molecules in pristine Zn(tbip), but were unable to find transition states for this process with activation energies less than 3 eV. This observation is in agreement with the expectations from the pore dimensions that diffusion of alkanes in defect-free Zn(tbip) should be single-file. The experiments of Heinke et al.,[31]

however, gave strong evidence for mutual passage via their transient concentration profile results. Since molecular diffusion in pristine Zn(tbip) is inconsistent with the experimental observations, we considered whether point defects in the MOF's pores could account for the observed behavior.

Table 1. Binding energies and diffusion energy barriers (kJ/mol) of C2-C4 alkanes in 1D channels of pristine Zn(tbip).

	Binding energy	Energy Barrier
C_2H_6	-36.7	7.5
C_3H_8	-44.8	23.6
n-C_4H_{10}	-57.7	28.9

Motivated by the point defects that are accessible in defect engineering of MOFs[11, 42-45], we considered linker vacancy (LV) defects in which the resulting unsaturated chemical bonds associated with a missing linker are terminated by water molecules or hydroxyl groups. Defects of this type could potentially arise during the initial synthesis of a MOF crystal or during later exposure to ambient conditions. The defect formation energy, ΔE, for a defect of this kind can be written as

$$\Delta E = E_{defect\ MOF} + mE_{H_2L} - E_{pristine\ MOF} - nE_{H_2O} \quad (1)$$

where $E_{defect\ MOF}$, E_{H_2L}, $E_{pristine\ MOF}$ and E_{H_2O} are the energy of the MOF with a linker vacancy defect, a protonated tbip linker, the defect-free MOF and an isolated water molecule, respectively, and m and n are stoichiometric coefficients.[12] An illustration of various aspects of linker vacancy (LV) defects in Zn(tbip) is shown in **Fig. 1**. Creating one LV defect in Zn(tbip) involves four Zn-O bond breaking events (**Fig. 1(a)**). After linker removal from the unit cell, two

hydrogen ions are assumed to protonate the linker and two pairs of a water molecule and a hydroxyl group that are hydrogen bonded to each other are assumed to terminate the Zn sites (**Fig. 1(b)**).

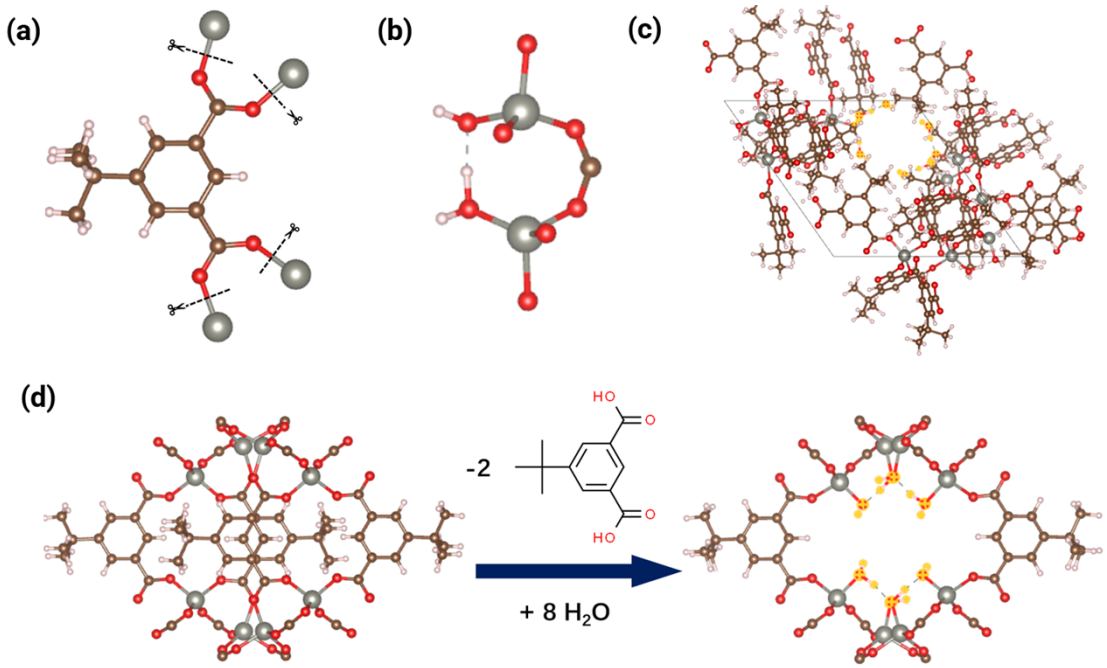

Figure 1. (a) Four Zn-O bond breaking events are needed to create one LV defect in Zn(tbip). (b) Zn sites are terminated with hydrogen-bonded water and hydroxyl groups after linker removal. (c) Two LV defects in a Zn(tbip) unit cell connecting adjacent 1D channels, with terminating water and hydroxyl groups highlighted in yellow. (d) The overall process of creating a pair of LV defects in a Zn(tbip) unit cell.

We also considered the formation of two adjacent LV defects as shown in **Fig. 1(d)**. We assume that the two resulting LV defects are formed in a stepwise manner. This gave the following formation energies for the formation energies of two LV defects, where E_{1LV} and E_{2LV} are the energies of Zn(tbip) with 1 and 2 LV defects:

$$\Delta E_{1st\,LV} = E_{1LV} + E_{H_2L} - E_{pristine} - 4E_{H_2O} = 0.46\ eV \quad (2)$$

$$\Delta E_{2nd\,LV} = E_{2LV} + E_{H_2L} - E_{1LV} - 4E_{H_2O} = 0.19\ eV \quad (3)$$

It is notable that the formation energy for a single defect is moderate, suggesting that the existence of these defects in materials that have been synthesized and activated at moderate temperatures is plausible. This defect formation energy is smaller than the analogous result that the 0.57 eV formation energy has been reported for ZIF-8 using the same DFT functional.[12]

A striking aspect of these results is that the formation energy of the second LV defect is lower than the formation energy for the first defect due to the additional hydrogen bonds between the terminated water and hydroxyl groups when the second defect is formed (see **Fig. S1**). We also partially investigated the energy of forming a third LV defect using two examples (see **Fig. S2**). The formation energies of a third LV defect, 0.13 eV and 0.16 eV, are also lower than that of the first LV. A similar although less pronounced observation was made by Han et al. for clustering of LV defects in ZIF-8.[12] These calculations indicate that defects made up of 2 LVs and more complex defects are likely to exist in Zn(tbip) under any conditions where formation of isolated LVs is physically feasible. Below, we examine the impacts on molecular diffusion on the 2 LV defects to understand whether these defects can account for the experimental observations of Heinke et al.[31]

An interesting observation about the adjacent LV defects defined above is that they create an opening that connects two adjacent 1D pores (see **Fig. S3**). Detailed examination of these configurations showed that this inter-pore connection has two distinct channels that could potentially allow molecules to move between 1D pores, as illustrated schematically in **Fig. 2**. To understand whether these defect-induced pore connections could account with the molecular

diffusion reported experimentally,[31] we examined molecular diffusion of ethane, propane and butane using cNEB calculations. Initial and final configurations for cNEB calculations were optimized by placing guest molecules inside 1D channels and in channels created by LV defects. Multiple initial configurations were used for each binding energy calculation and the configurations with the most favorable energies were picked as the initial and final image for cNEB calculations.

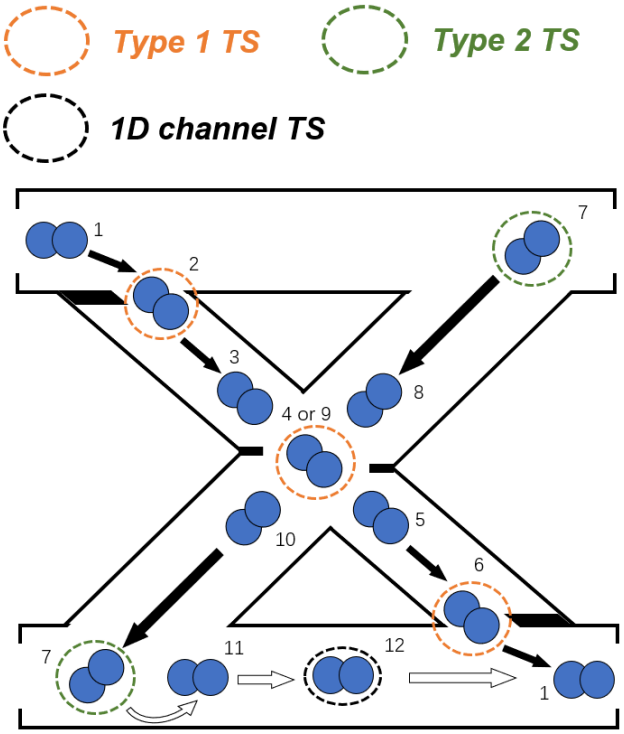

Figure 2. Illustration of two 1D pores in Zn(tbip) (top and bottom) connected via an opening created by an adjacent pair of linker vacancy defects. The defects allow two distinct connections between the 1D channels, shown as type 1 (top left to bottom right) and type 2 (top right to bottom left). Energy minima and transition states for diffusing molecules are shown, with transition states indicated with dashed ovals. The structure shown in the connecting channels is intended to illustrate the complexity of these paths, not to highlight specific structural features of the MOF.

An overview of molecular diffusion inside Zn(tbip) with an adjacent pair of LV defects is shown in **Fig. 2**. We first consider the path between adjacent pores denoted as Type 1 in **Fig. 2**. The potential energy surface for ethane, propane, and butane in this channel is shown quantitatively in **Fig. 3**. For each molecule, binding is more favorable in the vicinity of the defects (sites 3 and 5) than in the 1D channel and the largest energy barrier is associated with hopping from these sites into the 1D channel. The resulting rate-controlling energy barrier for ethane, propane, and butane is 17.8, 26.2, and 26.9 kJ/mol, respectively (See **Table 2**). For ethane and propane these barriers are larger than for diffusion along the pristine 1D channel listed in **Table 1**, but they are small enough that these processes would occur readily at moderate temperatures.

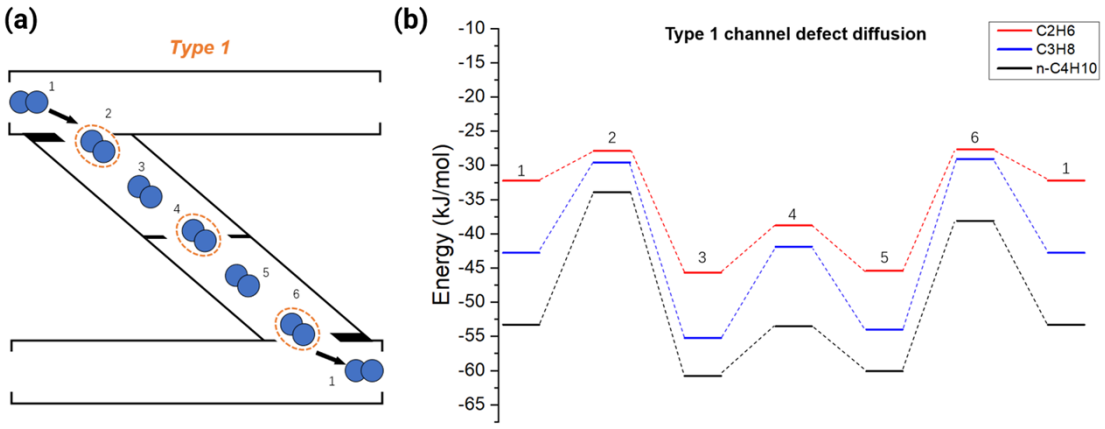

Figure 3. (a) Illustration of Type 1 channel defect diffusion with transition states of each diffusion step indicated with a dashed circle. (b) Energies of the states shown in (a) for ethane, propane, and butane.

The Type 2 channel has a lower overall energy barrier for all three alkanes compared to Type 1 (see **Fig. 4**). Similar as the Type 1 channel, the rate determining step is hopping from the defect

window into the 1D channel (image 7). When a guest molecule is diffusing inside 1D channel and encounter a Type 2 channel, it will first rotate to enter the channel into defect binding sites (from image 7 to 8), followed by a similar step as in Type 1 to travel to the other side of the defect window (image 8 to 10) and diffuse back into 1D channel due to symmetricity (image 10 to 7).

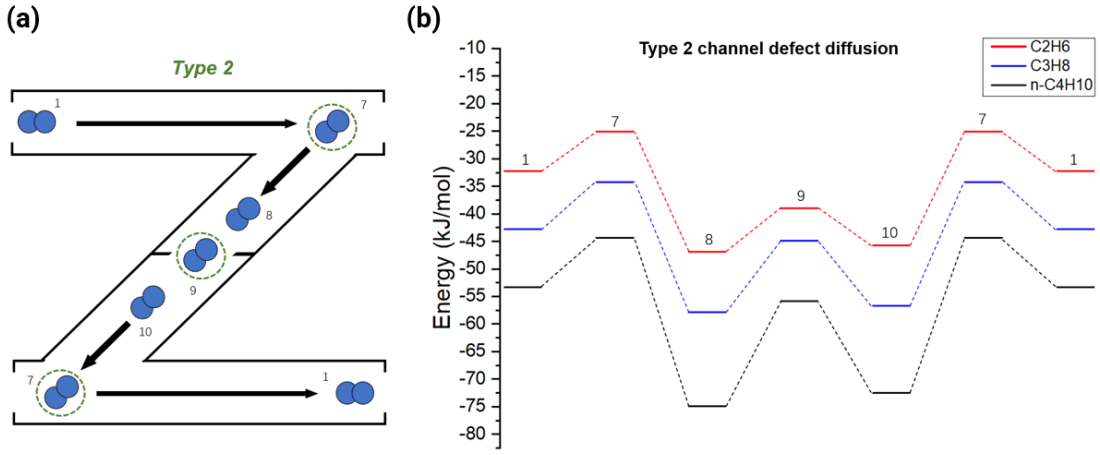

Figure 4. (a) Illustration of Type 2 channel defect diffusion with image corresponds to the energy states calculated in (b). Transition states of each diffusion step are highlighted with dashed circle.

The description above focused on molecular hopping between adjacent 1D channels. It is also important to understand the implication of the defects on diffusion along 1D channels. This situation is illustrated in **Fig. 5**, where the numbering of the local minima and transition states is consistent with **Fig. 2**. The net energy barriers for ethane, propane and n-butane diffusion past the pair of defects are 3.9, 18.4 and 21.7 kJ/mol, compared to diffusion barriers of 7.5, 23.6 and 28.7 kJ/mol, respectively in the pristine 1D pore (see **Table 2**). These observations suggest that

the presence of the LV defects will not significantly impede diffusion along 1D channels relative to the defect-free material.

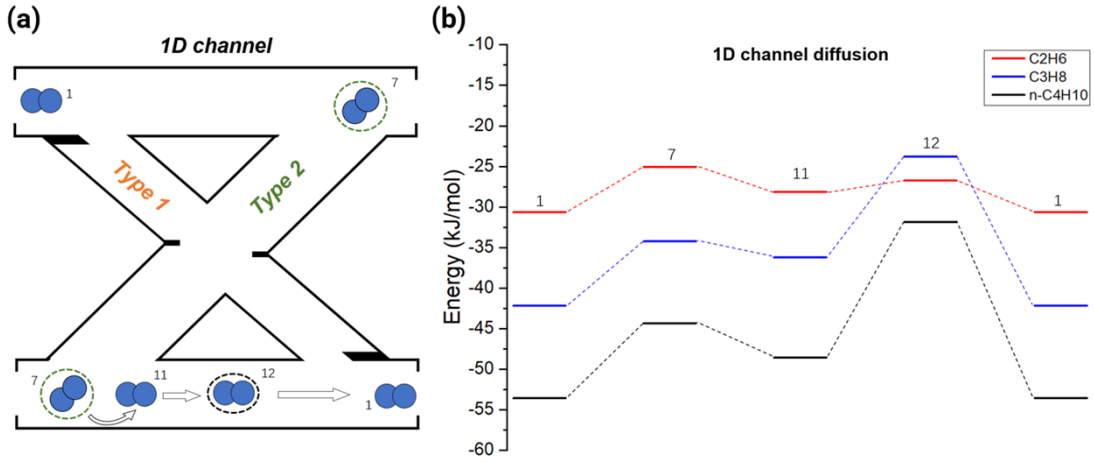

Figure 5. (a) Illustration of 1D channel diffusion past a pair of LV defects and (b) computed energy for each local minimum and transition state noted in (a).

Table 2. Diffusion energy barrier of the rate determining step and the global optimal binding sites (Type 2) in three types of channels in Zn(tbip) with 2 LV defects.

	Energy barrier (kJ/mol)				B.E. (kJ/mol)
	Type 1	Type 2	1D channel (LV defects)	1D channel (Pristine)	Type 2
C_2H_6	17.8	21.9	3.93	7.5	-46.9
C_3H_8	26.2	23.6	18.4	23.6	-57.9
n-C_4H_{10}	26.9	30.6	21.7	28.9	-74.9

Combining our observations of defect formation energies and diffusion energy barrier gives strong indications that the mutual passages in Zn(tbip) discovered by Heinke et al.[31] were caused

by point defects presented in the crystals used experimentally. It is possible that defects made up of more than two linker vacancies could also contribute to the experimentally observed diffusion, but the presence of defects created by pairs of linker vacancies is sufficient to account for the experimental outcome without further contributions from more complex defects.

Pore blockage defects inside Zn(tbip)

Another observation from Heinke et al.[32] using a microkinetic model was that diffusion of short-chain alkanes in Zn(tbip) is controlled by transport resistances at the MOF crystal's external surface, also called a surface barrier. Analysis based on this microkinetic model suggested that most of the MOFs 1D pores were blocked, preventing direct entry of guest molecules. Here, we explore whether the existence of LV defects might explain the previous interpretation of experimental observations in terms of surface barriers. Our results indicate that pore blockages associated with linker fragments from formation of LV defects could play an important role in molecular diffusion in Zn(tbip), although these blockages are not specifically associated with the external surface of the MOF crystals.

When a LV defect form inside a MOF crystal, it is commonly assumed the linkers are removed from the structure[46-49]. Here, we consider an alternative scenario in which a hydrolyzed tbip linker remains inside the MOF, creating the possibility that it will block the transport of guest molecules in Zn(tbip). We refer these kinds of defects as pore blockage (PB) defects in the following discussion. DFT optimization was performed by placing a hydrolyzed tbip linker inside a pristine Zn(tbip) 1D channel and a NEB calculation was used to determine the diffusion energy barrier inside the 1D channel. This calculation gave a diffusion energy barrier of 127

kJ/mol, suggesting that at moderate temperatures the mobility of isolated hydrolyzed linkers would be very slow. Binding energy of one tbip linker inside a pristine 1D channel was determined to be -62 kJ/mol. The scenario just described assumes that a PB defect is created by formation of a LV defect and subsequent movement of the hydrolyzed linker along the 1D pore away from the site of the LV defect. The strong binding energy indicates that the desorption rate of the linker will be very slow even if it overcomes the large internal diffusion barriers to travel to the surface of the crystal.

Our DFT calculations indicated that both LV defects and PB defects could exist inside Zn(tbip) at experimentally accessible conditions. The actual defect concentrations in the samples used in Heinke et al.'s experiments [31] is not known, but it seems plausible to assume that PB defects will have a lower concentration than LV defects since PB defects are formed from incomplete removal of linkers from the structure. Critically, however, one PB defect can completely block a 1D channel for molecular diffusion, so even a dilute concentration of these defects would lead to the same conclusion as Heinke et al.'s microkinetic model that most of the pores are blocked. We emphasize that this process has nothing to do with the external surface of the MOF crystal, so it is not strictly correct to refer to it as a surface barrier.

An overview of the mechanism for alkane diffusion in Zn(tbip) implied by our results is shown in **Fig. 6**, which shows a far higher density of defects that is likely in a real MOF for clarity. Long range diffusion along a single 1D pore is blocked by PB defects (shown as black vertical bars in **Fig. 6**), but the presence of pairs of LV defects allows molecules to switch between adjacent 1D channels. This description is consistent with the lack of single-file diffusion

observed experimentally and also the indication from experimental data of phenomena that prevent molecules from directly entering many 1D channels.

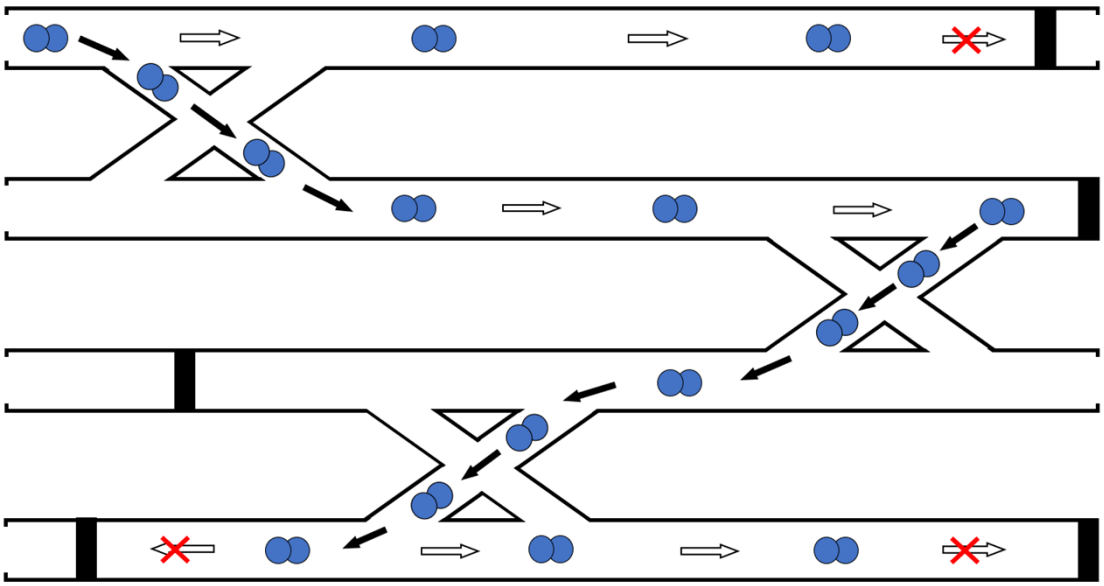

Figure 6. Molecular diffusion behavior in a schematic illustration of Zn(tbip) containing both LV defects (shown connecting adjacent 1D channels) and PB defects (shown as black vertical bars). The density of defects shown in much higher than would be expected in a real material.

Conclusion

In this work we performed extensive DFT calculations to explore how defect formation associated with the presence of adsorbed water effect C_2H_6, C_3H_8 and *n*-C_4H_{10} diffusion in Zn(tbip), a MOF that in its pristine form as 1D channels that would lead to single-file diffusion for these molecules. Previous experiments showed strong evidence that adjacent 1D channels in Zn(tbip) are connected to each other for molecular diffusion[31], but no underlying mechanism was previously proposed. We examined pairs of linker vacancy (LV) defects in Zn(tbip), finding that the formation energy of these defects is reduced for adjacent defects, in agreement with similar

observations for ZIF-8 by Han et al.[12] Crucially, the existence of a point defect pair in Zn(tbip) opens two intersecting channels connecting adjacent 1D channels. Our DFT calculations predict that all three short-chain alkanes have diffusion energy barriers through these connecting pores channels that allow molecular hopping to occur readily at moderate temperature. These observations strongly suggest that the mutual passages in Zn(tbip) observed experimentally were caused by defects in the MOF structure.

A second surprising finding from the experiments of Heinke et al.[32] was the inference that most of Zn(tbip) 1D pores were blocked. We used DFT calculations to explore the influence of of hydrolyzed linker that would be created by the formation of LV defects inside the MOF's pores. Our calculations indicate the while formation of LV defects by adsorbed water is relatively favorable, diffusion of the resulting linker fragments and desorption of these fragments from the MOF's pores is likely to be very slow under experimentally-relevant conditions. Our calculations also show that these linkers effectively block pristine 1D pores for diffusion of alkanes. Thus, the formation of LV defects allowing molecules to hop between pores that are not connected in the pristine MOF and the blockage of many pores for diffusion over extended distances are closely connected for this MOF. Although the blockage of pores in Zn(tbip) had previously been described as a surface barrier, the description that emerges from our calculations shows that the blockages are not in fact associated with the external surface of the MOF, so this name is not strictly correct.

Our results provide, for the first time, a mechanistic description of the previously surprising diffusion characteristics of molecules in the 1D pores of Zn(tbip). There may be situations in

which this kind of defect-enabled diffusion is of practical use. A key feature of single-file diffusion is that the mobility of all species in a chemical mixture subject to single-file diffusion is reduced to approximately the mobility of the slowest moving species. This means that a material with strictly single-file diffusion cannot be used for kinetic separations. The defect-mediated hopping between 1D pores that occurs in Zn(tbip) provides a mixing mechanism that overcomes this limitation. There are a very large number of MOFs with 1D pores, so the possibility of deliberately using defects to improve the diffusion characteristics of these materials is intriguing.

ASSOCIATED CONTENT

Supporting Information

Potential energy surface results of short-chain alkanes diffusion in Zn(tbip) with a pair of LV defects, termination groups of LV defects formation, and illustration of two defect channels created from a pair of LV defects (PDF)

A total number of 18 VASP input files including 14 structure files of DFT optimized structures of defect-free Zn(tbip) and Zn(tbip) with up to three LV defects; global binding sites of short-chain alkanes in Zn(tbip) with a pair of LV defects; Zn(tbip) with one PB defect (ZIP)

AUTHOR INFORMATION

Corresponding Author

David S. Sholl − *Oak Ridge National Laboratory, Oak Ridge, TN 37830, United States;*

orcid.org/0000-0002-2771-9168; Phone: +1-404-894-2822; Email: shollds@ornl.gov

Author

Xuqing Cai - School of Chemical & Biomolecular Engineering, Georgia Institute of Technology, Atlanta, GA 30332, United States

ACKNOWLEDGMENT

This work was supported by the Dow Chemical Company. Helpful discussions with Dr. Hanjun Fang at Georgia Tech are greatly appreciated.

REFERENCES

(1) Furukawa, H.; Cordova, K. E.; O'Keeffe, M.; Yaghi, O. M. The chemistry and applications of metal-organic frameworks. *Science* **2013**, *341* (6149), 1230444.

(2) Herm, Z. R.; Bloch, E. D.; Long, J. R. Hydrocarbon Separations in Metal–Organic Frameworks. *Chemistry of Materials* **2013**, *26* (1), 323-338.

(3) You, W.; Sen, T.; Kawajiri, Y.; Realff, M. J.; Sholl, D. S. Using Site Heterogeneity in Metal–Organic Frameworks with Bimetallic Open Metal Sites for Olefin/Paraffin Separations. *ACS Applied Nano Materials* **2020**, *3* (6), 5291-5300.

(4) You, W.; Liu, Y.; Howe, J. D.; Sholl, D. S. Competitive Binding of Ethylene, Water, and Carbon Monoxide in Metal–Organic Framework Materials with Open Cu Sites. *The Journal of Physical Chemistry C* **2018**, *122* (16), 8960-8966.

(5) Sholl, D. S.; Lively, R. P. Defects in Metal-Organic Frameworks: Challenge or Opportunity? *J Phys Chem Lett* **2015**, *6* (17), 3437-3444.

(6) Zhou, K.; Mousavi, B.; Luo, Z.; Phatanasri, S.; Chaemchuen, S.; Verpoort, F. Characterization and properties of Zn/Co zeolitic imidazolate frameworks vs. ZIF-8 and ZIF-67. *Journal of Materials Chemistry A* **2017**, *5* (3), 952-957.

(7) Ameloot, R.; Vermoortele, F.; Hofkens, J.; De Schryver, F. C.; De Vos, D. E.; Roeffaers, M. B. Three-dimensional visualization of defects formed during the synthesis of metal-organic frameworks: a fluorescence microscopy study. *Angew Chem Int Ed Engl* **2013**, *52* (1), 401-405.

(8) St Petkov, P.; Vayssilov, G. N.; Liu, J.; Shekhah, O.; Wang, Y.; Woll, C.; Heine, T. Defects in MOFs: a thorough characterization. *Chemphyschem* **2012**, *13* (8), 2025-2029.

(9) Cheetham, A. K.; Bennett, T. D.; Coudert, F. X.; Goodwin, A. L. Defects and disorder in metal organic frameworks. *Dalton Trans* **2016**, *45* (10), 4113-4126.

(10) Cliffe, M. J.; Wan, W.; Zou, X.; Chater, P. A.; Kleppe, A. K.; Tucker, M. G.; Wilhelm, H.; Funnell, N. P.; Coudert, F. X.; Goodwin, A. L. Correlated defect nanoregions in a metal-organic framework. *Nat Commun* **2014**, *5*, 4176.

(11) Zhang, C.; Han, C.; Sholl, D. S.; Schmidt, J. R. Computational Characterization of Defects in Metal-Organic Frameworks: Spontaneous and Water-Induced Point Defects in ZIF-8. *J Phys Chem Lett* **2016**, *7* (3), 459-464.

(12) Han, R.; Tymińska, N.; Schmidt, J. R.; Sholl, D. S. Propagation of Degradation-Induced Defects in Zeolitic Imidazolate Frameworks. *The Journal of Physical Chemistry C* **2019**, *123* (11), 6655-6666.

(13) Bhattacharyya, S.; Han, R.; Joshi, J. N.; Zhu, G.; Lively, R. P.; Walton, K. S.; Sholl, D. S.; Nair, S. Stability of Zeolitic Imidazolate Frameworks in NO2. *The Journal of Physical Chemistry C* **2019**, *123* (4), 2336-2346.

(14) Han, R.; Sholl, D. S. Computational Model and Characterization of Stacking Faults in ZIF-8 Polymorphs. *The Journal of Physical Chemistry C* **2016**, *120* (48), 27380-27388.

(15) Willhammar, T.; Sun, J.; Wan, W.; Oleynikov, P.; Zhang, D.; Zou, X.; Moliner, M.; Gonzalez, J.; Martinez, C.; Rey, F.; et al. Structure and catalytic properties of the most complex intergrown zeolite ITQ-39 determined by electron crystallography. *Nat Chem* **2012**, *4* (3), 188-194.

(16) Fang, Z.; Bueken, B.; De Vos, D. E.; Fischer, R. A. Defect-Engineered Metal-Organic Frameworks. *Angew Chem Int Ed Engl* **2015**, *54* (25), 7234-7254.

(17) Van Speybroeck, V.; Vandenhaute, S.; Hoffman, A. E. J.; Rogge, S. M. J. Towards modeling spatiotemporal processes in metal–organic frameworks. *Trends in Chemistry* **2021**, *3* (8), 605-619.

(18) Shearer, G. C.; Chavan, S.; Bordiga, S.; Svelle, S.; Olsbye, U.; Lillerud, K. P. Defect Engineering: Tuning the Porosity and Composition of the Metal–Organic Framework UiO-66 via Modulated Synthesis. *Chemistry of Materials* **2016**, *28* (11), 3749-3761.

(19) Vermoortele, F.; Bueken, B.; Le Bars, G.; Van de Voorde, B.; Vandichel, M.; Houthoofd, K.; Vimont, A.; Daturi, M.; Waroquier, M.; Van Speybroeck, V.; et al. Synthesis modulation as a tool to increase the catalytic activity of metal-organic frameworks: the unique case of UiO-66(Zr). *J Am Chem Soc* **2013**, *135* (31), 11465-11468.

(20) Feng, X.; Hajek, J.; Jena, H. S.; Wang, G.; Veerapandian, S. K. P.; Morent, R.; De Geyter, N.; Leyssens, K.; Hoffman, A. E. J.; Meynen, V.; et al. Engineering a Highly Defective Stable UiO-66 with Tunable Lewis- Bronsted Acidity: The Role of the Hemilabile Linker. *J Am Chem Soc* **2020**, *142* (6), 3174-3183.

(21) Verploegh, R. J.; Nair, S.; Sholl, D. S. Temperature and Loading-Dependent Diffusion of Light Hydrocarbons in ZIF-8 as Predicted Through Fully Flexible Molecular Simulations. *J Am Chem Soc* **2015**, *137* (50), 15760-15771.

(22) Yang, Y.; Sholl, D. S. A systematic examination of the impacts of MOF flexibility on intracrystalline molecular diffusivities. *Journal of Materials Chemistry A* **2022**, *10* (8), 4242-4253.

(23) Sharp, C. H.; Bukowski, B. C.; Li, H.; Johnson, E. M.; Ilic, S.; Morris, A. J.; Gersappe, D.; Snurr, R. Q.; Morris, J. R. Nanoconfinement and mass transport in metal-organic frameworks. *Chem Soc Rev* **2021**, *50* (20), 11530-11558.

(24) Han, C.; Verploegh, R. J.; Sholl, D. S. Assessing the Impact of Point Defects on Molecular Diffusion in ZIF-8 Using Molecular Simulations. *J Phys Chem Lett* **2018**, *9* (14), 4037-4044.

(25) Heinke, L.; Wöll, C. Surface ‐ Mounted Metal ‐ Organic Frameworks: Surface ‐ Mounted Metal ‐ Organic Frameworks: Crystalline and Porous Molecular Assemblies for Fundamental Insights and Advanced Applications (Adv. Mater. 26/2019). *Advanced Materials* **2019**, *31* (26).

(26) Iacomi, P.; Formalik, F.; Marreiros, J.; Shang, J.; Rogacka, J.; Mohmeyer, A.; Behrens, P.; Ameloot, R.; Kuchta, B.; Llewellyn, P. L. Role of Structural Defects in the Adsorption and Separation of C3 Hydrocarbons in Zr-Fumarate-MOF (MOF-801). *Chemistry of Materials* **2019**, *31* (20), 8413-8423.

(27) Pan, L.; Parker, B.; Huang, X.; Olson, D. H.; Lee, J.; Li, J. Zn(tbip) (H2tbip= 5-tert-butyl isophthalic acid): a highly stable guest-free microporous metal organic framework with unique gas separation capability. *J Am Chem Soc* **2006**, *128* (13), 4180-4181.

(28) Simon, C. M.; Mercado, R.; Schnell, S. K.; Smit, B.; Haranczyk, M. What Are the Best Materials To Separate a Xenon/Krypton Mixture? *Chemistry of Materials* **2015**, *27* (12), 4459-4475.

(29) Hahn, K.; Karger, J.; Kukla, V. V. Single-file diffusion observation. *Phys Rev Lett* **1996**, *76* (15), 2762-2765.

(30) Gupta, V.; Nivarthi, S. S.; McCormick, A. V.; Ted Davis, H. Evidence for single file diffusion of ethane in the molecular sieve AlPO4-5. *Chemical Physics Letters* **1995**, *247* (4-6), 596-600.

(31) Heinke, L.; Tzoulaki, D.; Chmelik, C.; Hibbe, F.; van Baten, J. M.; Lim, H.; Li, J.; Krishna, R.; Karger, J. Assessing guest diffusivities in porous hosts from transient concentration profiles. *Phys Rev Lett* **2009**, *102* (6), 065901.

(32) Heinke, L.; Karger, J. Correlating surface permeability with intracrystalline diffusivity in nanoporous solids. *Phys Rev Lett* **2011**, *106* (7), 074501.

(33) Sholl, D. S. Metal-organic frameworks: a porous maze. *Nat Chem* **2011**, *3* (6), 429-430.

(34) Knio, O.; Fang, H.; Boulfelfel, S. E.; Nair, S.; Sholl, D. S. Molecular Dynamics Investigation of Surface Resistances in Zeolite Nanosheets. *The Journal of Physical Chemistry C* **2020**, *124* (28), 15241-15252.

(35) Hibbe, F.; Chmelik, C.; Heinke, L.; Pramanik, S.; Li, J.; Ruthven, D. M.; Tzoulaki, D.; Karger, J. The nature of surface barriers on nanoporous solids explored by microimaging of transient guest distributions. *J Am Chem Soc* **2011**, *133* (9), 2804-2807.

(36) Zimmermann, N. E. R.; Zabel, T. J.; Keil, F. J. Transport into Nanosheets: Diffusion Equations Put to Test. *The Journal of Physical Chemistry C* **2013**, *117* (14), 7384-7390.

(37) Zimmermann, N. E. R.; Smit, B.; Keil, F. J. Predicting Local Transport Coefficients at Solid–Gas Interfaces. *The Journal of Physical Chemistry C* **2012**, *116* (35), 18878-18883.

(38) Kresse, G.; Furthmuller, J. Efficient iterative schemes for ab initio total-energy calculations using a plane-wave basis set. *Phys Rev B Condens Matter* **1996**, *54* (16), 11169-11186.

(39) Grimme, S.; Antony, J.; Ehrlich, S.; Krieg, H. A consistent and accurate ab initio parametrization of density functional dispersion correction (DFT-D) for the 94 elements H-Pu. *J Chem Phys* **2010**, *132* (15), 154104.

(40) Henkelman, G.; Uberuaga, B. P.; Jónsson, H. A climbing image nudged elastic band method for finding saddle points and minimum energy paths. *The Journal of Chemical Physics* **2000**, *113* (22), 9901-9904.

(41) Sheppard, D.; Terrell, R.; Henkelman, G. Optimization methods for finding minimum energy paths. *J Chem Phys* **2008**, *128* (13), 134106.

(42) Yuan, L.; Tian, M.; Lan, J.; Cao, X.; Wang, X.; Chai, Z.; Gibson, J. K.; Shi, W. Defect engineering in metal-organic frameworks: a new strategy to develop applicable actinide sorbents. *Chem Commun (Camb)* **2018**, *54* (4), 370-373.

(43) Hardian, R.; Dissegna, S.; Ullrich, A.; Llewellyn, P. L.; Coulet, M. V.; Fischer, R. A. Tuning the Properties of MOF-808 via Defect Engineering and Metal Nanoparticle Encapsulation. *Chemistry* **2021**, *27* (22), 6804-6814.

(44) Wu, D.; Yan, W.; Xu, H.; Zhang, E.; Li, Q. Defect engineering of Mn-based MOFs with rod-shaped building units by organic linker fragmentation. *Inorganica Chimica Acta* **2017**, *460*, 93-98.

(45) Taddei, M.; Schukraft, G. M.; Warwick, M. E. A.; Tiana, D.; McPherson, M. J.; Jones, D. R.; Petit, C. Band gap modulation in zirconium-based metal–organic frameworks by defect engineering. *Journal of Materials Chemistry A* **2019**, *7* (41), 23781-23786.

(46) Tu, B.; Pang, Q.; Wu, D.; Song, Y.; Weng, L.; Li, Q. Ordered vacancies and their chemistry in metal-organic frameworks. *J Am Chem Soc* **2014**, *136* (41), 14465-14471.

(47) Chong, S.; Thiele, G.; Kim, J. Excavating hidden adsorption sites in metal-organic frameworks using rational defect engineering. *Nat Commun* **2017**, *8* (1), 1539.

(48) Pang, Q.; Yang, L.; Li, Q. Vacancies in Metal−Organic Frameworks: Formation, Arrangement, and Functions. *Small Structures* **2022**.

(49) Gutov, O. V.; Gonzalez Hevia, M.; Escudero-Adan, E. C.; Shafir, A. Metal-Organic Framework (MOF) Defects under Control: Insights into the Missing Linker Sites and Their Implication in the Reactivity of Zirconium-Based Frameworks. *Inorg Chem* **2015**, *54* (17), 8396-8400.

TOC Graphic